

Article

Observation of Structural Diversity Based on the Cationic Influence in a Series of Zn/Cd Pyridine Carboxylate Coordination Compounds

Rupam Sen ^{1,*}, Abhishek Banerjee ¹, Paula Brandão ²  and Zhi Lin ^{2,*} ¹ Department of Chemistry, Adamas University, Barasat, Kolkata 700126, India² Department of Chemistry, CICECO, University of Aveiro, 3810-193 Aveiro, Portugal

* Correspondence: rupamsen1@yahoo.com (R.S.); zlin@ua.pt (Z.L.)

Abstract: In this study, we used a 6-methyl-2,3-pyridine dicarboxylate ligand to develop the frameworks. Two novel compounds, $[\text{Zn}_2(\text{L})_2(\text{H}_2\text{O})_4]$ (**1**) and $[\text{Cd}(\text{L})(\text{H}_2\text{O})]$ (**2**) (where L = 6-methylpyridine-2,3-dicarboxylate) were produced. The compounds were characterized by elemental analysis, powder X-ray diffraction, Fourier-transform infrared spectroscopy and single crystal X-ray crystallography. We successfully tuned the framework dimensionality by varying the size of the metal ions from small Zn to large Cd ions. Single crystal X-ray investigations of compound **1** show a good dimeric motif, while compound **2** shows a 2D network. In compound **1**, the dimeric units are further bonded by strong hydrogen bonds and create a 3D network whereas compound **2** produces a 2D layer that in turn connects via short contacts to form a 3D network in the crystallographic space.

Keywords: hydrothermal synthesis; coordination polymer; crystal structure; cation size effect



Citation: Sen, R.; Banerjee, A.; Brandão, P.; Lin, Z. Observation of Structural Diversity Based on the Cationic Influence in a Series of Zn/Cd Pyridine Carboxylate Coordination Compounds. *Crystals* **2023**, *13*, 186. <https://doi.org/10.3390/cryst13020186>

Academic Editor: Alexander Y. Nazarenko

Received: 28 December 2022

Revised: 12 January 2023

Accepted: 18 January 2023

Published: 20 January 2023



Copyright: © 2023 by the authors. Licensee MDPI, Basel, Switzerland. This article is an open access article distributed under the terms and conditions of the Creative Commons Attribution (CC BY) license (<https://creativecommons.org/licenses/by/4.0/>).

1. Introduction

Molecular designing has now extended to vastly varied fields of intricacy and has considerably matured, developing a rich knowledge and control over the molecular design of structures. The field of molecular and supramolecular crystal engineering has attracted much attention because of the divergent geometry and from the perspectives of the exploration of novel multi-functional compounds, introducing different bridging organic linkers and metal ions [1]. The molecular self-assembly process is involved in the interaction of the metal ions and ligands with enough structural information and many interesting self-assembly frameworks have been developed and cited in the literature [2]. Understanding and controlling the external factors that influence the crystallization process and overall stability of crystals, such as metal coordinating nature, temperature, pH and solvent, are essential to creating the required network with unique functionality. By maintaining the same reaction mixture at varied temperatures, Cheetham and co-workers published a systematic investigation of the impact of temperature on the production of the distinct cobalt carboxylate phases [3]. Rao et al. successfully established the temperature-controlled progressive assembling of Zn oxalate and Ni succinate systems [4]. Mahata et al. provided a stunning illustration of temperature- and time-controlled coordination framework synthesis in a different publication [5]. Maji et al. synthesized 1D to 3D frameworks by only varying the reaction temperature [6].

The pH and temperature of the reaction medium are not the only important factors to developing different framework solids; coordinating the nature of the metal ions also has a significant impact on the dimensionality of the compounds [7]. As we go down the periodic table, the size of the metal ions also changes gradually and hence the nature of the coordination also changes. Bigger ions can accommodate more ligands and hence influence the dimensionality of the frameworks.

It is crucial to note that the scientific community continues to pay special attention to the Zn(II) and Cd(II) metal-organic frameworks (MOFs), which have intriguing adsorptive, catalytic and sensing capabilities. The high adsorption capacities [8,9], luminous [10–12] and nonlinear optical (NLO) [13–15] features of these coordination polymers should be highlighted with priority. Zn (II) and Cd (II) ions are different in their atomic radii and coordination strengths, yet they share the same d^{10} electronic configuration from the perspective of crystal engineering. The enormous number of homoligand and mixed-ligand coordination networks, which include both isostructural and isomorphous analogues, may provide strong justification for this. In the present study, we developed two frameworks, $[Zn_2(L)_2(H_2O)_4]$ (**1**) and $[Cd(L)(H_2O)]_n$ (**2**), with the L = 6-methyl pyridine-2,3-dicarboxylate ligand. Their structures were studied. Depending on the metal ions, the dimensionality of coordination networks changes from a dimeric unit to a 2D structure.

2. Materials and Methods

2.1. Synthetic Methodology

Numerous reports on different methods of synthesizing MOFs have been collated so far in the literature. The most widely used method is the conventional hydro/solvothermal synthesis, which involves heating the reaction mixture by the means of electrical heating. In most cases, the crystals are grown inside the reactor by monitoring the reactant concentration, volume of the solvents and reaction temperature. In the present study, we followed the hydrothermal technique to produce the desired single crystalline compounds. It is noteworthy that the N/O-containing heterocyclic carboxylic acids are of immense importance in producing metal-organic frameworks with different dimensionalities. Recently, a variety of coordination frameworks has been developed by using the heterocyclic carboxylate ligands. It is worth mentioning that the heterocyclic carboxylic acids are very sensitive towards external incitements (such as pH, temperature, solvent, etc.) in producing divergent topological frameworks [16]. In our recent work, we successfully modulated framework dimensionality by changing the pH of the medium using a N-heterocyclic carboxylate system [17]. Maji et al. produced a series of frameworks using N-heterocyclic carboxylate ligands by varying the temperature [6]. Ghosh et al. developed a series of Zn-based O-heterocyclic carboxylate frameworks with diverse dimensionalities by alteration of the reaction temperature [18]. In the present study, we prepared a series of Zn/Cd-based dicarboxylate systems by varying the metal ion radius. The O-heterocyclic carboxylate can adopt different bridging modes to successfully construct a different molecular framework. It is worth mentioning that the deliberate change in metal ion radius is also an effective method for designing and building coordination compounds. Furthermore, it is notable that Zn/Cd have attracted extensive interest as metal centres for the construction of MOFs, featuring important photoluminescence properties and, more fascinatingly, Cd ions can adopt a variety of coordination numbers from four to seven in common [19]. Because of their several coordination geometries, they can adopt different topological networks. Here, in the present work we found a nice dimeric moiety in compound **1** and a 2D network for compound **2**. Both the compounds possess hydrogen bonding to produce a 3D structure.

2.2. Synthesis of Compounds **1** and **2**

6-Methylpyridine-2,3-dicarboxylic acid was purchased from Sigma and used as received. $Cd(NO_3)_2$, $Zn(NO_3)_2$ and solvents were procured from Merck (India). Compounds **1** and **2** were crystallized as colourless crystals in the Teflon-lined acid digestion bomb. The reaction mixtures were kept at 160 °C for 3 days then cooled to room temperature. For digestion, $Zn(NO_3)_2 \cdot 6H_2O$ or $Cd(NO_3)_2 \cdot 4H_2O$ and 6-Methylpyridine-2,3-dicarboxylic acid were mixed in a 1:1 ratio in water and the pH was maintained at 6 by adding aqueous KOH solution. The crystals obtained were washed by H_2O and ethanol, dried in ambient temperature and finally kept in a desiccator. The calculated yields were 38% and 41% for compounds **1** and **2**, respectively (based on carboxylic acid).

2.3. Characterization of Compounds 1 and 2

To evaluate the structure of the compounds, various techniques were used. Elemental analysis, Fourier-transform infrared spectroscopy (FT-IR), powder X-ray diffraction (PXRD) and single-crystal X-ray diffraction were employed for these purposes.

2.3.1. Elemental Analysis

Elemental analysis was performed to establish the formula of the compounds. CHN analysis was conducted with a Thermo Scientific Flash 2000 instrument. The results, given in Table 1, clearly indicate the phase purity of the compounds.

Table 1. Elemental analysis of compounds 1 and 2.

%	Calculated		Found	
	1	2	1	2
C	34.22	31.05	34.92	30.75
H	3.20	2.28	3.32	2.85
N	4.99	4.52	4.89	4.97

2.3.2. Fourier-Transform Infrared (FT-IR) Spectroscopy

The FT-IR spectra (4000–400 cm^{-1}) were recorded on powdered samples suspended in KBr pellet and collected on a Thermo Scientific Nicolet 6700 apparatus. The FT-IR spectra of compounds 1 and 2 are given in Figure 1. Selected IR peaks are found at 1655, 1592 [$\bar{\nu}_{\text{as}}(\text{CO}_2^-)$], 1476 [$\bar{\nu}_{\text{s}}(\text{CO}_2^-)$], 1371, 1340 [$\bar{\nu}_{\text{s}}(\text{C-O})$] and 3400–3000 s.br [$\bar{\nu}(\text{O-H})$] cm^{-1} for compound 1 and at 1633, 1594 [$\bar{\nu}_{\text{as}}(\text{CO}_2^-)$], 1539 [$\bar{\nu}_{\text{s}}(\text{CO}_2^-)$], 1479, 1400 [$\bar{\nu}_{\text{s}}(\text{C-O})$] and weak 3400–3000 s.br [$\bar{\nu}(\text{O-H})$] cm^{-1} for compound 2. The literature reports indicated that 6-methylpyridine-2,3-dicarboxylic acid generates bands at ca. 3452, 3019, 2908, 1731, 1368, 1610, 839 cm^{-1} . The band intensities changed after MOF formation, and depended on the MOF structures [20,21].

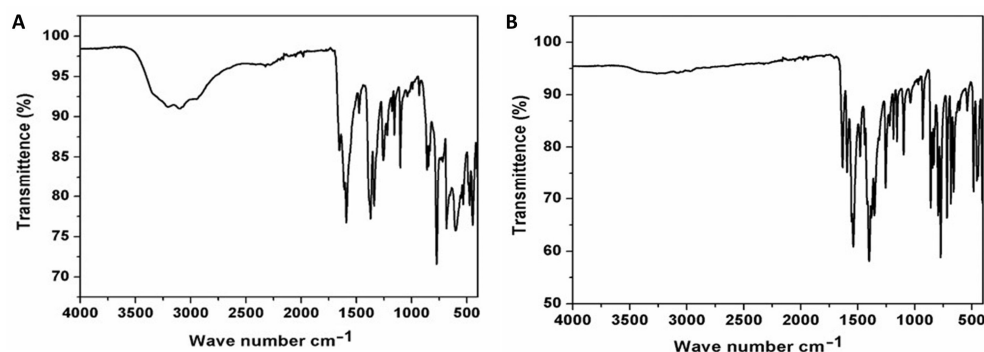


Figure 1. Fourier-transform infrared spectra of compounds 1 (A) and 2 (B).

2.3.3. Powder and Single-Crystal X-ray Crystallographic Studies

Bruker SMART APEX CCD X-ray diffractometer was used to collect X-ray diffraction data. Data were collected at 293(2) K using graphite-monochromated $\text{MoK}\alpha$ radiation ($\lambda = 0.71073 \text{ \AA}$). SAINT software package [22] was used to determine the integrated intensities and cell refinement was performed using a narrow-frame integration algorithm. Empirical absorption correction was applied (SADABS) [23] on the collected data. Using direct method, the structures were solved in SHELXT 2014/5 and refined using full-matrix least-square technique against F^2 with anisotropic displacement parameters for non-hydrogen atoms using SHELXL2018/3 [24]. All the hydrogen atoms were located from the difference Fourier map and refined isotopically. The refinement parameters and summary of crystal data for compounds 1 and 2 have been collated in Table 2 and selected bond distances and angles have been collated in Table 3.

Table 2. Summary of crystal data and refinement parameters for compounds **1** and **2**.

Compound	1	2
Formula	C ₁₆ H ₁₈ N ₂ O ₁₂ Zn ₂	C ₈ H ₇ NO ₅ Cd
Formula Weight	561.06	309.56
Temperature (K)	293(2)	293(2)
Wavelength (Å)	0.71073	0.71073
Crystal System	Monoclinic	Triclinic
Space group	P2 ₁ /c	P $\bar{1}$
a (Å)	7.1923(4)	7.3698(2)
b (Å)	14.7691(8)	7.9846(2)
c (Å)	8.8998(5)	8.0498(2)
α, β, γ (°)	90, 93.487(2), 90	94.969(10), 106.898(10), 105.817(10)
Volume (Å ³)	943.62(9)	428.942(19)
Calculated density (g·cm ⁻³)	1.975	2.397
Z	2	1
θ range for data collection (°)	2.68–30.60	2.69–33.27
F(000)	568	300
Absorption coefficient (mm ⁻¹)	2.616	2.545
Unique reflections	2906	3286
R ₁ , wR ₂ [I > 2 σ (I)]	0.0221, 0.0568	0.0166, 0.0395
Goodness of fit (S)	1.066	1.051

$$R_1 = \frac{\sum ||F_o| - |F_c||}{\sum |F_o|}, wR_2 = \left[\frac{\sum w(|F_o| - |F_c|)^2}{\sum w(F_o^2)} \right]^{\frac{1}{2}}$$

Table 3. Selected bond lengths (Å) and angles (°) for compounds **1** and **2**.

Bond Lengths (Å)		Bond Angles (°)	
Compound 1			
Zn1–O1	1.989(1)	O1–Zn1–O4	120.78(5)
Zn1–O4	1.966(1)	O1–Zn1–N1	78.67(5)
Zn1–N1	2.166(1)	O1–Zn1–O3	84.08(5)
Zn1–O3	2.133(1)	O1–Zn1–O5	135.47(5)
Zn1–O5	1.988(1)	O3–Zn1–O5	91.08(5)
Compound 2			
Cd1–O1	2.2581(10)	O5–Cd1–O4 ⁱⁱ	87.43(4)
Cd1–O5	2.2884(10)	N1–Cd1–O4 ⁱⁱ	86.31(4)
Cd1–N1	2.3108(11)	O3 ⁱ –Cd1–O4 ⁱⁱ	118.63(4)
Cd1–O3 ⁱ	2.3678(10)	O1–Cd1–O4 ⁱ	149.92(4)
Cd1–O4 ⁱⁱ	2.4183(11)	O5–Cd1–O4 ⁱ	73.56(4)
Cd1–O4 ⁱ	2.5031(11)	N1–Cd1–O4 ⁱ	113.99(4)
Cd1–O2 ⁱⁱⁱ	2.5553(11)	O3 ⁱ –Cd1–O4 ⁱ	53.47(3)
O1–Cd1–O5	94.33(4)	O4 ⁱⁱ –Cd1–O4 ⁱ	67.18(4)
O1–Cd1–N1	73.99(4)	O1–Cd1–O2 ⁱⁱⁱ	77.66(3)
O5–Cd1–N1	167.16(4)	O5–Cd1–O2 ⁱⁱⁱ	80.44(4)
O1–Cd1–O3 ⁱ	156.02(4)	N1–Cd1–O2 ⁱⁱⁱ	101.71(4)
O5–Cd1–O3 ⁱ	89.78(4)	O3 ⁱ –Cd1–O2 ⁱⁱⁱ	79.76(3)
N1–Cd1–O3 ⁱ	103.06(4)	O4 ⁱⁱ –Cd1–O2 ⁱⁱⁱ	158.08(4)
O1–Cd1–O4 ⁱⁱ	85.19(4)	O4 ⁱ –Cd1–O2 ⁱⁱⁱ	125.32(3)

$$^{(i)} x, -1 + y, z; ^{(ii)} -x, 1 - y, 1 - z; ^{(iii)} 1 - x, 1 - y, 1 - z.$$

Powder X-ray diffraction of compounds **1** and **2** was performed at room temperature on a PANalytical Empyrean diffractometer in a Bragg–Brentano geometry using CuK α X-radiation (1.5418 Å) with 2θ range between 10° and 50°. The simulated powder patterns were calculated from single crystal X-ray diffraction data using program Powder Cell [25]. The PXRD patterns, given in Figures S1 and S2, indicated that compound **1** is quite pure while compound **2** seems to have impurities.

3. Results

3.1. Structural Description of Compound $[Zn_2(L)_2(H_2O)_4]$ (1)

Compound 1 crystallizes in the space group $P2_1/c$ with the z value of 2. The asymmetric unit contains one Zn(II) ion, one deprotonated ligand and two water molecules. In the simplest unit, the Zn(II) centres are in trigonal bipyramid (TBP) geometry. The basal plane of the TBP is formed by two carboxylate oxygen atoms (O1 and O3) and one water molecule (O6), while the apical positions are occupied by one water molecule (O5) and one pyridyl nitrogen atom (N1). An ORTEP view of compound 1 with atom numbering scheme is shown in Figure 2a. The Zn–O and Zn–N bond distances are 1.966–2.133 and 2.166 Å, respectively, which are in accordance with the previous report [26]. In the whole structure of 1, two zinc(II) centres are bridged by the pyridyl carboxylate anions to form a porous dimeric structure (Figure 2b). These dimeric units are further linked by hydrogen bonding in the 3D crystallographic space. The extra stability in the compound is gained by the strong hydrogen bonding in all the 3D space (Figure 3 and Table S1). The geometry of the Zn ion was determined by continuous shape measurement using the program SHAPE 2.1 [27]. This measurement can give deviations from minimal distortion paths and polyhedral interconversion generalized coordinates. The analysis results of the Zn ion in compound 1, listed in Table 4, indicated that TBP gives the smallest deviations. Therefore, the Zn ion in compound 1 can be considered as adopting TBP geometry with D_{3h} symmetry and the continuous shape measure (CSHM) value of 2.391. However, it is also not far from “spherical square pyramid” geometry with C_{4v} symmetry since the CSHM value is 2.724.

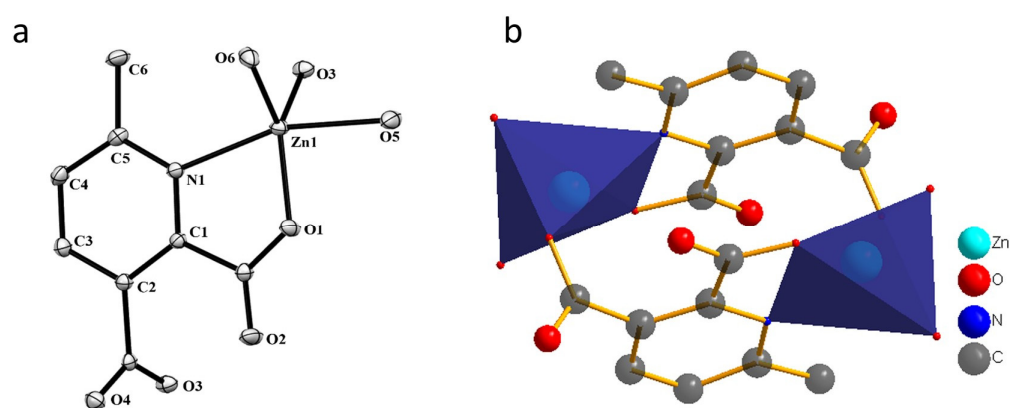


Figure 2. (a) The ORTEP view with atom numbering scheme and with 40% ellipsoid probability and (b) Dimeric unit for compound 1. H atoms are omitted for clarity.

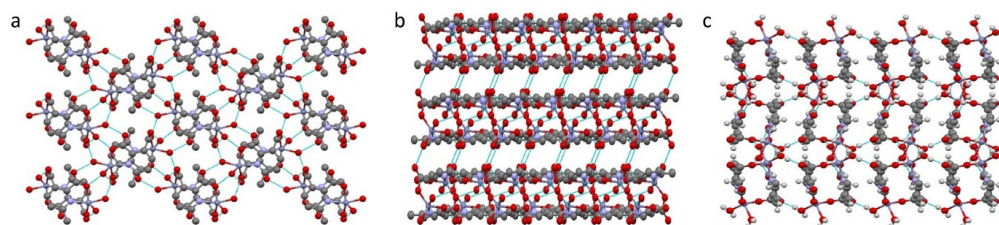


Figure 3. Hydrogen bonds in compound 1, viewed along a -axis (a), b -axis (b) and c -axis (c).

Table 4. The continuous shape measure of the Zn ion in compound 1.

Polyhedron Shape	Symmetry	CSHM Value
Pentagon	D_{5h}	28.454
Vacant octahedron	C_{4v}	4.061
Trigonal bipyramid	D_{3h}	2.391
Spherical square pyramid	C_{4v}	2.724
Johnson trigonal bipyramid J12	D_{3h}	3.975

Hirshfeld surface (HS) analysis is a useful tool for presenting and visualizing the intermolecular short contact in molecular crystals [28]. The HS and related fingerprint plots in this work were calculated using the program Crystal Explorer [29]. The quantification of the interactions between the atoms within the molecular crystal was illustrated via a colour gradient. The red spots indicate the short interatomic contacts, while the white and blue areas show contacts with the distance among the atoms equal to or greater than the sum of the Van der Waals radii of the atoms. The HS of compound **1** plotted over d_{norm} in Figure 4 clearly shows the red spots, indicating the strong H-bonding interaction. The characteristics and type of intermolecular interactions in molecular crystals were represented by 2D fingerprint plots (Figure 5), which give the percentage contribution of each contact. The d_i is the distance from the HS to the nearest atom I internal to the surface, the d_e is the distance from the HS to the nearest atom E external to the surface, while the d_{norm} is the normalized sum of d_e and d_i [26]. Figure 5 clearly shows that the main intermolecular interactions in the molecular packing of compound **1** come from O...H and H...H short contacts. The contribution of H...O contact is the most significant (59.9%), which is attributed to the O—H...O and C—H...O hydrogen bonds. H...H contact contributes 28.4%. Therefore, compound **1** gets extra stability in three-dimensional crystallographic space through hydrogen bonding; there are two kinds of hydrogen bonds, strong O—H...O hydrogen bonds and comparatively weaker C—H...O hydrogen bonds. Strong hydrogen bonds form between the coordinated water molecules and carboxylate oxygen atoms [30]. There are four types of hydrogen bonds among the water molecules and carboxylate oxygen atoms. These are: O5—H5A...O3 with a D—A distance of 2.8420(15) Å with an angle of 173(2)°; O5—H5B...O2 with a D—A distance of 2.8066(15) Å with an angle of 178(3)°; O6—H6D...O1 with a D—A distance of 2.6743(15) Å with an angle of 175(2)°; O6—H6E...O1 with a D—A distance of 2.6278(15) Å with an angle of 171(3)°. There are a few non-classical hydrogen bonds with longer D—A distances and also the angles deviate more from 180 degrees, namely: C3—H3...O4 with a D—A distance of 3.2009(17) Å with an angle of 131°; C6—H6A...O4 with a D—A distance of 3.4562(19) Å with an angle of 169°; C3—H6B...O4 with a D—A distance of 3.4997(18) Å with an angle of 162°; C3—H6C...O4 with a D—A distance of 3.3576(18) Å with an angle of 135°. Hydrogen bonding plays the key important role in growing the compound in a three-dimensional space [31].

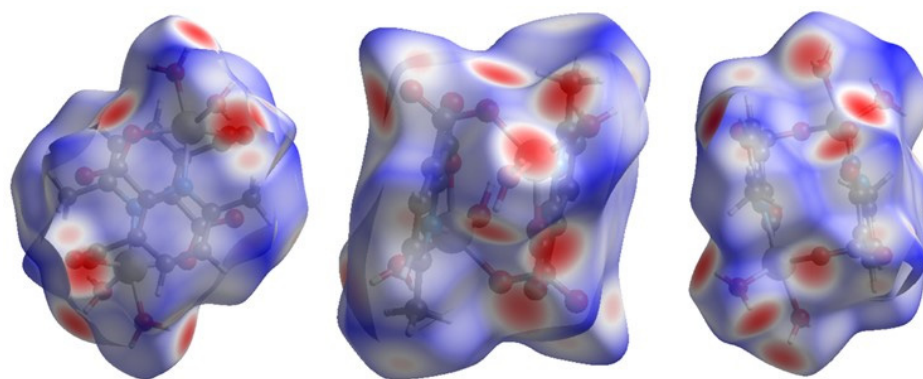


Figure 4. Hirshfeld surface of compound **1** plotted over d_{norm} in the range -0.742 (red) to 1.307 (blue) a.u., view in three directions.

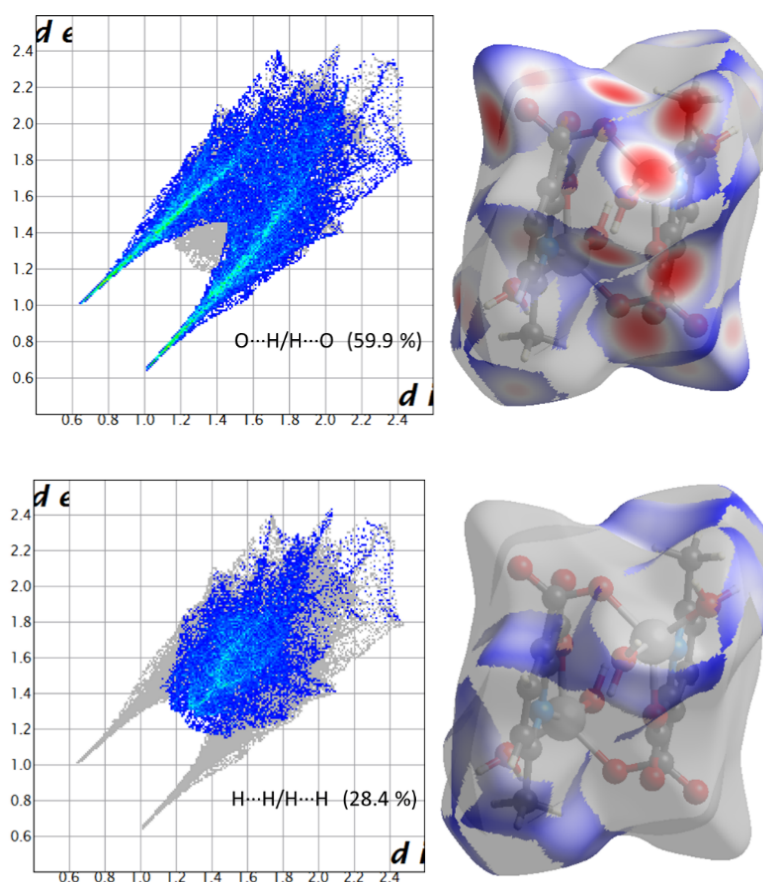


Figure 5. Fingerprint plots showing the contributions of specific interacting pairs (blue areas) in the whole plot (grey). Surface maps (right ones) indicate the applicable areas (in blue) that are associated with the specific intermolecular contact(s) in compound **1**.

3.2. Structural Description of Compound $[Cd(L)(H_2O)]_n$ (**2**)

Compound **2** crystallizes in the space group $P\bar{1}$ with the z value of 1. The asymmetric unit contains a single Cd(II) ion, one ligand and one water molecule. In the structure of compound **2**, the Cd(II) ion is seven coordinated, adopting capped octahedron geometry. The ORTEP diagram with atom numbering scheme is shown in Figure 6. The basal plane of the CdX_7 polyhedron is formed by one pyridyl nitrogen atom (N1), two carboxylate oxygen atoms (O4 and O2) and one water molecule (O5), while the axial positions are occupied by the two *syn-anti* carboxylate oxygen atoms (O3 and O1); the capped position is fulfilled by one carboxylate *syn-syn* bridging oxygen atom (O4[#]). The Cd–O and Cd–N bond distances are 2.258–2.555 and 2.311 Å, respectively, which are in accord with the previous report [32]. The two Cd are bridged by the *syn-anti* bridging carboxylate to form a Cd_2 dyad, which in turn is bridged by another carboxylate to form a two-dimensional plane (Figure 7). The crystallographic packing is shown in Figure 8 and the hydrogen bonding detail is collated in Table S2. Along the a -axis, the pores of the framework can be seen. The continuous shape measurement results, listed in Table 5, indicate that the “pentagonal bipyramid” gives the smallest deviations. Therefore, the Cd ion can be considered as adopting “pentagonal bipyramid” geometry with D_{5h} symmetry and the CShM value of 3.689. However, it is also not far from “capped trigonal prism” geometry with C_{2v} symmetry since the CShM value is 3.703. Figure 9 visualizes the H-bonding interaction in compound **2**. The red colour in Figure 9 is much lighter than that in Figure 4 of compound **1**, which indicates a weaker short contact interaction than that in compound **1**. Figure 10 gives the percentage contribution of each contact. The main interactions also come from H...O (38.6%) and H...H contacts (23.9%). However, C...H contact also contributes 16.0%. The 2D networks

extends its dimensionality in 3D crystallographic space through hydrogen bonding. The extra stability is gained by hydrogen bonding between carboxylate oxygen atoms and coordinated water molecules. The hydrogen bonds include O5—H5A···O3 with a D—A distance of 2.6636(18) Å with an angle of 162(2)°; O5—H5B···O2 with a D—A distance of 2.8370(15) Å with an angle of 152(3)°; O5—H5B···O4 with a D—A distance of 2.8741(17) Å with an angle of 111(2)°. The non-classical hydrogen bonding includes C6—H6A···O5 with a D—A distance of 3.4505(19) Å with an angle of 159°; C6—H6B···O5 with a D—A distance of 3.5277(17) Å with an angle of 160°; C6—H6C···O5 with a D—A distance of 3.2522(19) Å with an angle of 132°; all the hydrogen bonds contribute to increase the overall stability of the compound **2** [30,31].

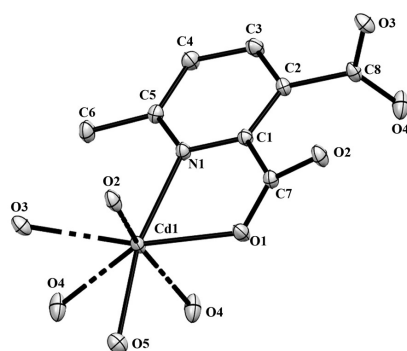


Figure 6. The ORTEP view of compound **2** with atom numbering scheme and with 40% ellipsoid probability (H atoms are omitted for clarity).

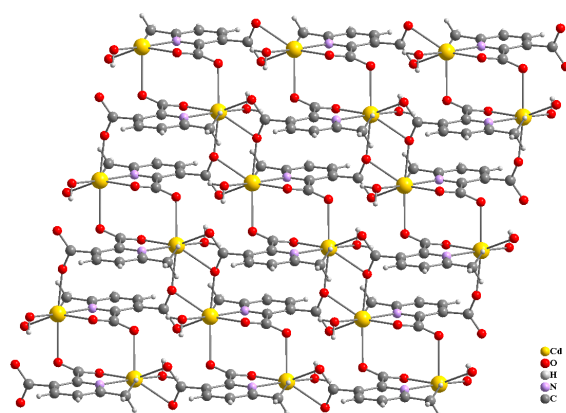


Figure 7. Propagation of the compound **2** in *ab*-plane.

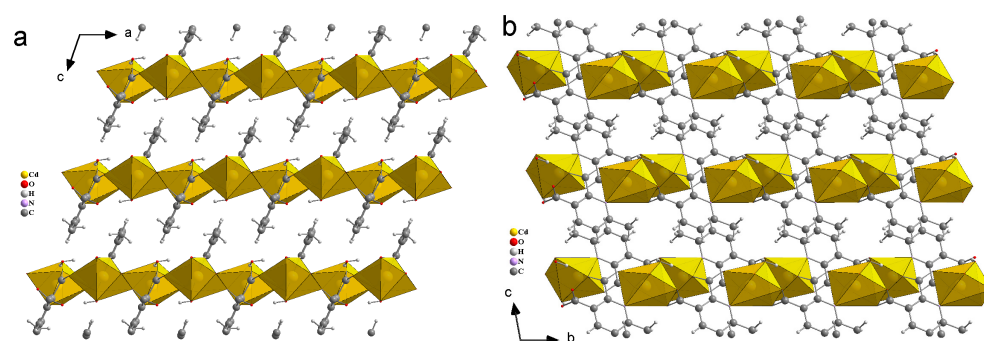


Figure 8. Three-dimensional packing of compound **2**, viewed along *b*-axis (a), *a*-axis (b).

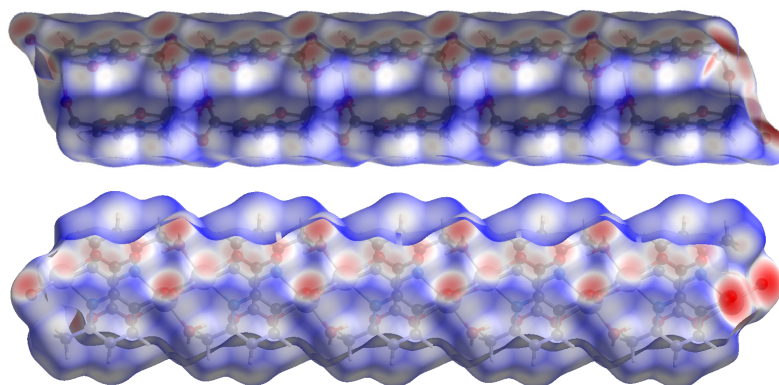


Figure 9. Hirshfeld surface plotted over d_{norm} in the range -1.209 (red) to 1.042 (blue) a.u. view in two directions for compound 2.

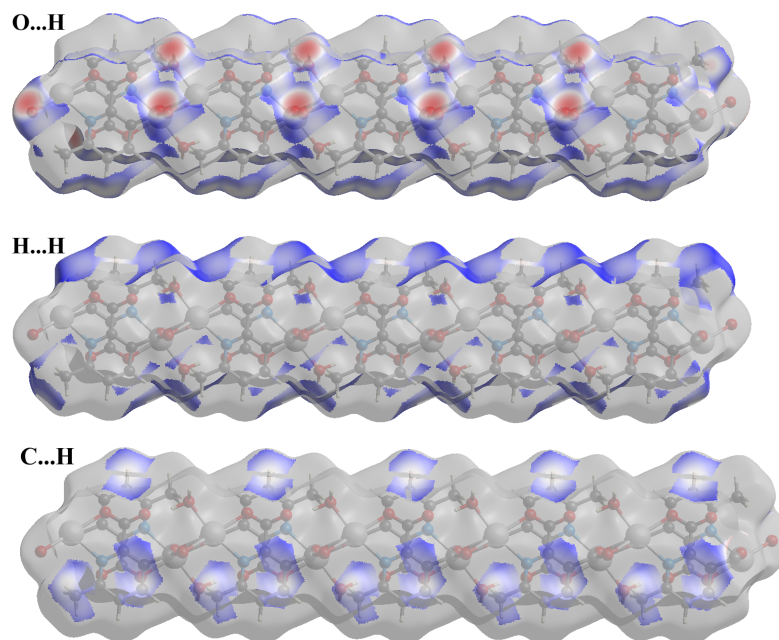
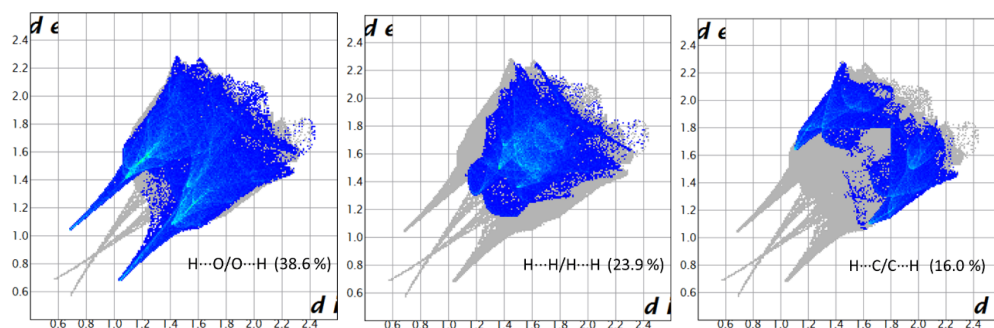


Figure 10. Fingerprint plots of compound 2, showing the contributions of specific interacting pairs. Surface maps indicate the applicable areas. The colour settings are the same as Figure 5.

Table 5. The continuous shape measure of the Cd ion in compound 2.

Polyhedron Shape	Symmetry	CSHM Value
Heptagon	D _{7h}	28.604
Hexagonal pyramid	C _{6v}	19.347
Pentagonal bipyramid	D _{5h}	3.689
Capped octahedron	C _{3v}	5.047
Capped trigonal prism	C _{2v}	3.703
Johnson pentagonal bipyramid J13	D _{5h}	6.495
Johnson elongated triangular pyramid J7	C _{3v}	19.422

Little research has been performed using the 6-methyl-2,3-pyridine dicarboxylate ligand with Zn and Co metal ions. Wei et al. performed a synthesis at 80 °C for 3 days in the mixed solvent of water and DMF [20]. In the resulting compound, the 6-methyl-2,3-pyridine dicarboxylate ligands bridged Zn(II), forming a one-dimensional chain. Zn (II) is in octahedron with two water molecules. These chains form a three-dimensional stacking via a hydrogen bonding interaction and Van der Waals forces. In a mixed solvent of water, ethanol and DMF, Co(II) induces a compound with a very similar structure after 140 °C for 3 days [21]. With the second ligand, more sophisticated structures can be formed [33,34]. Gurunatha and Maji studied the synthesis with 1,2-bis-(4-pyridyl)ethylene as the second ligand and Fe, Co and Ni as metal ions in ambient temperature [33]. After 7 days, all three metal ions induced the same two-dimensional threefold interpenetrated supermolecules, in which the metal centre was in six coordination with two 6-methyl-2,3-pyridine dicarboxylate ligands and two 1,2-bis-(4-pyridyl)ethylene ligands. The 1,2-bis-(4-pyridyl)ethylene ligand does not connect fragments to each other to form a three-dimensional framework. The mononuclear fragments are connected to each other via hydrogen bonding. Wei et al. performed the synthesis with 1,10-phenanthroline as the second ligand and Cu as the metal ion at 80 °C for 3 days in a mixed solvent of water and methanol [34]. It resulted in a one-dimensional chain, which is somewhat similar to that of Wei's compound using Zn and without the second ligand [20], but the two water ligands are replaced by one 1,10-phenanthroline ligand.

4. Conclusions and Perspectives

Various parameters can influence the dimensionality of the coordination framework. In this study, we selected two metal ions fixing the ligand. We carefully moved from the first row to the second row in the periodic table. As we know, the radii increase down a group and the larger ions can accommodate more donating sites. Here, by varying the metal ions we encountered frameworks of different dimensionalities. Two compounds with 6-methyl-2,3-pyridine dicarboxylate ligands were prepared only by varying the metal ions from smaller Zn to larger Cd and keeping the same reaction condition. Compound 1 adopts a simple dimer with Zn as the central metal ion while compound 2 possesses an interesting 2D network with Cd as the central atom. The carboxylate bridged two Cd ions and formed a Cd₂ dyad. Both the compounds possess a hydrogen-bonded three-dimensional structure. We performed Hirshfeld Surface analysis to evaluate the intermolecular interaction. The analysis revealed the presence of strong intermolecular hydrogen bonding and short contacts. The contribution of H···O contact was found to be the most significant in crystal packing. In this way, we can develop different series of compounds with different dimensionality and hence with different physical and chemical properties. Considering the limited research on MOFs with the 6-methyl-2,3-pyridine dicarboxylate ligand, and the various structures obtained with different solvents and/or second ligands and/or different temperatures, more new frameworks may be obtained in future. In fact, the impurities indicated by the PXRD of the Cd sample showed this possibility. This area of study will open a new pathway for fabricating different frameworks possessing novel properties.

Supplementary Materials: The following supporting information can be downloaded at: <https://www.mdpi.com/article/10.3390/cryst13020186/s1>, Table S1. Hydrogen bonds present in compound 1; Table S2. Hydrogen bonds present in compound 2; Figure S1. Experimental and simulated (from single crystal X-ray diffraction data) powder X-ray diffraction of compound 1; Figure S2. Experimental and simulated (from single crystal X-ray diffraction data) powder X-ray diffraction of compound 2.

Author Contributions: The material synthesis, preliminary characterization was performed at Adamas University (R.S., A.B.). Crystal structure determination and structure analysis were performed at the University of Aveiro (P.B., Z.L.). All authors have read and agreed to the published version of the manuscript.

Funding: This research received no external funding.

Institutional Review Board Statement: Not applicable.

Informed Consent Statement: Not applicable.

Data Availability Statement: CCDC-2218250 and 2218251 contain the supplementary crystallographic data for these two compounds. These data can be obtained free of charge from The Cambridge Crystallographic Data Centre via www.ccdc.cam.ac.uk/data_request/cif (accessed on 8 November 2022).

Acknowledgments: R.S. thanks DST-SERB for the ECR grant (ECR/2016/001572) and Adamas University for financial support (AU/R&D/SEED/03/03-2020-21). The researchers from Aveiro acknowledge the project CICECO-Aveiro Institute of Materials, UIDB/50011/2020, UIDP/50011/2020 & LA/P/0006/2020, financed by national funds through the Portuguese Foundation for Science and Technology/MCTES.

Conflicts of Interest: The authors declare no conflict of interest.

References

1. Chan, M.H.-Y.; Yam, V.W.-W. Toward the Design and Construction of Supramolecular Functional Molecular Materials Based on Metal–Metal Interactions. *J. Am. Chem. Soc.* **2022**, *144*, 22805–22825. [[CrossRef](#)]
2. Lyu, D.; Xu, W.; Elise, J.; Payong, L.; Zhang, T.; Wang, Y. Low-dimensional assemblies of metal-organic framework particles and mutually coordinated anisotropy. *Nat. Commun.* **2022**, *13*, 3980. [[CrossRef](#)]
3. Forster, P.M.; Burbank, A.R.; Livage, C.; Férey, G.; Cheetham, A.K. The role of temperature in the synthesis of hybrid inorganic–organic materials: The example of cobalt succinates. *Chem. Commun.* **2004**, 368–369. [[CrossRef](#)]
4. Dan, M.; Rao, C.N.R. A building-up process in open-framework metal carboxylates that involves a progressive increase in dimensionality. *Angew. Chem. Int. Ed.* **2006**, *45*, 281–285. [[CrossRef](#)]
5. Mahata, P.; Sundaresan, A.; Natarajan, S. The role of temperature on the structure and dimensionality of MOFs: An illustrative study of the formation of manganese oxy-bis(benzoate) structures. *Chem. Commun.* **2007**, 4471–4473. [[CrossRef](#)]
6. Gurunatha, K.L.; Uemura, K.; Maji, T.K. Temperature- and Stoichiometry-Controlled Dimensionality in a Magnesium 4,5-Imidazolidicarboxylate System with Strong Hydrophilic Pore Surfaces. *Inorg. Chem.* **2008**, *47*, 6578–6580. [[CrossRef](#)]
7. Kang, J.; Abedin Khan, N.; Haque, E.; Jhung, S.H. Chemical and Thermal Stability of Isotypic Metal–Organic Frameworks: Effect of Metal Ions. *Chem. Eur. J.* **2011**, *17*, 6437–6442. [[CrossRef](#)]
8. Li, H.; Davis, C.E.; Groy, T.L.; Kelley, D.G.; Yaghi, O.M. Coordinatively Unsaturated Metal Centers in the Extended Porous Framework of Zn₃(BDC)₃·6CH₃OH (BDC=1,4-Benzenedicarboxylate). *J. Am. Chem. Soc.* **1998**, *120*, 2186–2187. [[CrossRef](#)]
9. Li, H.; Eddaoudi, M.; Groy, T.L.; Yaghi, O.M. Establishing Microporosity in Open Metal–Organic Frameworks: Gas Sorption Isotherms for Zn(BDC) (BDC=1,4-Benzenedicarboxylate). *J. Am. Chem. Soc.* **1998**, *120*, 8571–8572. [[CrossRef](#)]
10. Eddaoudi, M.; Li, H.; Reineke, T.; Fehr, M.; Kelley, D.; Groy, T.L.; Yaghi, O.M. Design and synthesis of metal-carboxylate frameworks with permanent microporosity. *Top. Catal.* **1999**, *9*, 105–111. [[CrossRef](#)]
11. Eddaoudi, M.; Li, H.; Yaghi, O.M. Highly Porous and Stable Metal–Organic Frameworks: Structure Design and Sorption Properties. *J. Am. Chem. Soc.* **2000**, *122*, 1391–1397. [[CrossRef](#)]
12. Eddaoudi, M.; Moler, D.B.; Li, H.; Chen, B.; Reineke, T.M.; ÖKeeffe, M.; Yaghi, O.M. Modular Chemistry: Secondary Building Units as a Basis for the Design of Highly Porous and Robust Metal–Organic Carboxylate Frameworks. *Acc. Chem. Res.* **2001**, *34*, 319–330. [[CrossRef](#)]
13. Pan, L.; Sander, M.B.; Huang, X.; Li, J.; Smith, M.; Bittner, E.; Bockrath, B.; Johnson, J.K. Microporous Metal Organic Materials: Promising Candidates as Sorbents for Hydrogen Storage. *J. Am. Chem. Soc.* **2004**, *126*, 1308–1309. [[CrossRef](#)]
14. Patel, N.; Shukla, P.; Lama, P.; Das, S.; Pal, T.K. Engineering of Metal–Organic Frameworks as Ratiometric Sensors. *Cryst. Growth Des.* **2022**, *22*, 3518–3564. [[CrossRef](#)]

15. Husain, A.; Ellwart, M.; Bourne, S.A.; Ohrström, L.; Oliver, C.L. Single-Crystal-to-Single-Crystal Transformation of a Novel 2-Fold Interpenetrated Cadmium–Organic Framework with Trimesate and 1,2-Bis(4-pyridyl)ethane into the Thermally Desolvated Form Which Exhibits Liquid and Gas Sorption Properties. *Cryst. Growth Des.* **2013**, *13*, 1526–1534. [[CrossRef](#)]
16. Wilson, J.A.; Uebler, J.W.; LaDuca, R.L. Cadmium adipate coordination polymers prepared with isomeric pyridylamide precursors: pH-dependent in situ reaction chemistry and divergent dimensionalities. *CrystEngComm* **2013**, *15*, 5218–5225. [[CrossRef](#)]
17. Sen, R.; Saha, D.; Koner, S. Controlled Construction of Metal–Organic Frameworks: Hydrothermal Synthesis, X-ray Structure, and Heterogeneous Catalytic Study. *Chem. Eur. J.* **2012**, *18*, 5979–5986. [[CrossRef](#)]
18. Nagarkar, S.S.; Chaudhari, A.K.; Ghosh, S.K. Bistable Dynamic Coordination Polymer Showing Reversible Structural and Functional Transformations. *Inorg. Chem.* **2012**, *51*, 8317–8321. [[CrossRef](#)]
19. Deng, Z.-P.; Huo, L.-H.; Qi, H.-L.; Zhu, L.-N.; Zhao, H.; Gao, S. Structural diversity of Zn(II)/Cd(II) complexes based on bis(pyridyl) ligands with a long flexible spacer: From zero-dimensional binuclear, one-dimensional chain, two-dimensional layer, to three-dimensional frameworks. *CrystEngComm* **2011**, *13*, 4218–4227. [[CrossRef](#)]
20. Wei, W.C.; Liu, Z.; Wei, R.Z.; Liang, C.X.; Feng, X.Z.; Han, G.C. Synthesis, crystal structure and anticorrosion performance of Zn(II) and Ni(II) complexes. *J. Mol. Struct.* **2021**, *1228*, 129452. [[CrossRef](#)]
21. Wei, R.Z.; Liu, Z.; Wei, W.C.; Liang, C.X.; Han, G.C.; Zhan, L. Synthesis, Crystal Structure and Characterization of Two Cobalt (II) Complexes Based on Pyridine Carboxylic Acid Ligands. *Z. Anorg. Allg. Chem.* **2022**, *648*, 83–88. [[CrossRef](#)]
22. Bruker. *APEX 2 SAINT XPREP*; Bruker AXS Inc.: Madison, WI, USA, 2007.
23. Bruker. *SADABS*; Bruker AXS Inc.: Madison, WI, USA, 2001.
24. Krause, L.; Herbst-Irmer, R.; Sheldrick, G.M.; Stalke, D. Comparison of silver and molybdenum microfocus X-ray sources for single-crystal structure determination. *J. Appl. Cryst.* **2015**, *48*, 3–10. [[CrossRef](#)]
25. Kraus, W.; Nolze, G. POWDER CELL—A Program for the Representation and Manipulation of Crystal Structures and Calculation of the Resulting X-ray Powder Patterns. *J. Appl. Crystallogr.* **1996**, *29*, 301–303. [[CrossRef](#)]
26. Mal, D.; Sen, R.; Brandão, P.; Lin, Z. Control formation of rigid linear and flexible zig-zig complexes based on Zn(II) and hydroxyquinoline carboxylate ligand system. *Inorg. Chem. Commun.* **2013**, *30*, 111–114. [[CrossRef](#)]
27. Alvarez, S.; Alemany, P.; Casanova, D.; Cirera, J.; Llunell, M.; Avnir, D. Shape maps and polyhedral interconversion paths in transition metal chemistry. *Coord. Chem. Rev.* **2005**, *249*, 1693–1708. [[CrossRef](#)]
28. Spackman, M.A.; Jayatilaka, D. Hirshfeld surface analysis. *CrystEngComm* **2009**, *11*, 19–32. [[CrossRef](#)]
29. Spackman, P.R.; Turner, M.J.; McKinnon, J.J.; Wolff, S.K.; Grimwood, D.J.; Jayatilaka, D.; Spackman, M.A. CrystalExplorer: A program for Hirshfeld surface analysis, visualization and quantitative analysis of molecular crystals. *J. Appl. Cryst.* **2021**, *54*, 1006–1011. [[CrossRef](#)]
30. Grabowski, S.J. Analysis of Hydrogen Bonds in Crystals. *Crystals* **2016**, *6*, 59. [[CrossRef](#)]
31. Sutor, D.J. The C–H . . . O hydrogen bond in crystals. *Nature* **1962**, *195*, 68–69. [[CrossRef](#)]
32. Mal, D.; Sen, R.; Brandão, P.; Shi, F.N.; Ferreira, R.A.S.; Lin, Z. Auxiliary ligand-assisted structural diversities of two coordination polymers with 2-hydroxyquinoline-4-carboxylic acid. *Inorg. Chem. Commun.* **2013**, *40*, 92–96. [[CrossRef](#)]
33. Gurunatha, K.L.; Maji, T.K. Three isomorphous threefold interpenetrated 2D supramolecular frameworks: Synthesis, structure and sorption properties. *Inorg. Chim. Acta* **2009**, *362*, 1541–1545. [[CrossRef](#)]
34. Wei, W.C.; Liu, Z.; Wei, R.Z.; Han, G.C.; Liang, C.X. Synthesis of MOFs/GO composite for corrosion resistance application on carbon steel. *RSC Adv.* **2020**, *10*, 29923–29934. [[CrossRef](#)]

Disclaimer/Publisher’s Note: The statements, opinions and data contained in all publications are solely those of the individual author(s) and contributor(s) and not of MDPI and/or the editor(s). MDPI and/or the editor(s) disclaim responsibility for any injury to people or property resulting from any ideas, methods, instructions or products referred to in the content.